doi:10.1093/brain/awm298 *Brain* (2008), **131**, 338–351

OPA1 mutations induce mitochondrial DNA instability and optic atrophy 'plus' phenotypes

Patrizia Amati-Bonneau,[1,2,*] Maria Lucia Valentino,[3,*] Pascal Reynier,[1,2] Maria Esther Gallardo,[4] Belén Bornstein,[4] Anne Boissière,[5] Yolanda Campos,[6] Henry Rivera,[6] Jesús González de la Aleja,[6] Rosanna Carroccia,[3] Luisa Iommarini,[3] Pierre Labauge,[7] Dominique Figarella-Branger,[8] Pascale Marcorelles,[9] Alain Furby,[10] Katell Beauvais,[10] Franck Letournel,[11] Rocco Liguori,[3] Chiara La Morgia,[3] Pasquale Montagna,[3] Maria Liguori,[12] Claudia Zanna,[13] Michela Rugolo,[13] Andrea Cossarizza,[14] Bernd Wissinger,[15] Christophe Verny,[16] Robert Schwarzenbacher,[17] Miguel Ángel Martín,[6] Joaquín Arenas,[6] Carmen Ayuso,[18] Rafael Garesse,[4] Guy Lenaers,[5] Dominique Bonneau[1,2] and Valerio Carelli[3]

[1]Département de Biochimie et Génétique, Centre Hospitalier Universitaire d'Angers, [2]INSERM U694, Angers, France, [3]Dipartimento di Scienze Neurologiche, Università di Bologna, Bologna, Italy, [4]Departamento de Bioquimica Instituto de Investigaciones Biomedicas 'Alberto Sols' CSIC-UAM, Facultad de Medicina, Universidad Autonoma de Madrid, CIBERER, ISCIII, Madrid, Spain, [5]INSERM U583, Institut des Neurosciences de Montpellier, Universités de Montpellier I et II, Montpellier, France, [6]Centro de Investigación, and Servicio de Neurología, Hospital Universitario 12 de Octubre, CIBERER, ISCIII, Madrid, Spain, [7]Service de Neurologie, Centre Hospitalier Universitaire de Nîmes, Nîmes, France, [8]Service d'Anatomie Pathologique et Neuropathologie, Centre Hospitalier Universitaire—Hopital de la Timone, Marseille, France, [9]Service d'Anatomie Pathologique, Centre Hospitalier Universitaire de Brest, Brest, France, [10]Service de Neurologie, Centre Hospitalier de Saint-Brieuc, Saint-Brieuc, France, [11]Laboratoire de Neurobiologie et Neuropathologie, Centre Hospitalier Universitaire d'Angers, Angers, France, [12]Institute of Neurological Sciences, National Research Council - Mangone, Cosenza, Italy, [13]Dipartimento di Biologia Evoluzionistica Sperimentale, Università di Bologna, Bologna, Italy, [14]Dipartimento di Scienze Biomediche, Sezione di Patologia Generale, Università di Modena e Reggio Emilia, Italy, [15]Molecular Genetics Laboratory, University Eye Hospital Tuebingen, Germany, [16]Département de Neurologie, Centre Hospitalier Universitaire d'Angers, Angers, France, [17]Structural Biology, University of Salzburg, Austria and [18]Servicio de Genética. Fundación Jiménez Díaz. CIBERER, ISCIII, Madrid, Spain

*These authors contributed equally to this study.

Correspondence to: Valerio Carelli, MD, PhD, Laboratorio di Neurogenetica, Dipartimento di Scienze Neurologiche, Università di Bologna, Via Ugo Foscolo 7, 40123, Bologna, Italy.
E-mail: valerio.carelli@unibo.it

Mutations in OPA1, a dynamin-related GTPase involved in mitochondrial fusion, cristae organization and control of apoptosis, have been linked to non-syndromic optic neuropathy transmitted as an autosomal-dominant trait (DOA). We here report on eight patients from six independent families showing that mutations in the *OPA1* gene can also be responsible for a syndromic form of DOA associated with sensorineural deafness, ataxia, axonal sensory-motor polyneuropathy, chronic progressive external ophthalmoplegia and mitochondrial myopathy with cytochrome *c* oxidase negative and Ragged Red Fibres. Most remarkably, we demonstrate that these patients all harboured multiple deletions of mitochondrial DNA (mtDNA) in their skeletal muscle, thus revealing an unrecognized role of the OPA1 protein in mtDNA stability. The five *OPA1* mutations associated with these DOA 'plus' phenotypes were all mis-sense point mutations affecting highly conserved amino acid positions and the nuclear genes previously known to induce mtDNA multiple deletions such as *POLG1*, *PEO1* (Twinkle) and *SLC25A4* (ANT1) were ruled out. Our results show that certain *OPA1* mutations exert a dominant negative effect responsible for multi-systemic disease, closely related to classical mitochondrial cytopathies, by a mechanism involving mtDNA instability.

Keywords: mitochondria; mtDNA multiple deletions; dominant optic atrophy; mitochondrial encephalomyopathy; chronic progressive external ophthalmoplegia

Abbreviations: BAEPs = brainstem auditory evoked potentials; BDLP = bacterial dynamin-like protein; CT = computerized tomography; CMT = Charcot–Marie-Tooth; COX = cytochrome c oxidase; CPEO = chronic progressive external ophthalmoplegia; DOA = dominant optic atrophy; FBS = fetal bovine serum; LHON = Leber's hereditary optic neuropathy; MEPs = motor evoked potentials; mtDNA = mitochondrial DNA; MRI = magnetic resonance imaging; MRS = MR spectroscopy; nDNA = nuclear DNA; OXPHOS = oxidative phosphorylation; PVEPs = pattern visual evoked potentials; RRFs = Ragged Red Fibres; SDH = succinate dehydrogenase; SEPs = somatosensorial evoked potentials; TP = thymidine phosphorylase

Received October 1, 2007. Revised November 7, 2007. Accepted November 16, 2007. Advance Access publication December 24, 2007

Mitochondrial disorders can be due to genetic defects in both the small mitochondrial double-stranded circular genome (mtDNA) and the nuclear DNA (DiMauro and Schon, 2003). A good example of this double genetic determination is represented by the two most frequent non-syndromic hereditary optic neuropathies, Leber's hereditary optic neuropathy (LHON; OMIM#535000) and dominant optic atrophy (DOA; OMIM#165500). LHON is due, in the large majority of worldwide cases, to one of three mtDNA point mutation at positions 11778/ND4, 3460/ND1 and 14484/ND6, all affecting different subunits of complex I (Carelli *et al.*, 2004). DOA, in about 60–70% of cases, is due to mutations in the nuclear gene encoding for the OPA1 protein (Alexander *et al.*, 2000; Delettre *et al.*, 2000; Cohn *et al.*, 2007), a dynamin-related GTPase targeted to mitochondria, which locates mostly on the mitochondrial inner membrane (Delettre *et al.*, 2002; Olichon *et al.*, 2006). OPA1 has been involved in multiple functions, the key role being the fusion of mitochondria and thus the mitochondrial network organization (Olichon *et al.*, 2006). Further OPA1 functions are oxidative phosphorylation (OXPHOS) and membrane potential maintenance (Olichon *et al.*, 2003; Lodi *et al.*, 2004; Amati-Bonneau *et al.*, 2005), as well as cristae organization and control of apoptosis through the compartimentalization of cytochrome *c* (Olichon *et al.*, 2003; Frezza *et al.*, 2006).

The large majority of mutations in the *OPA1* gene described to date are predicted to lead to a truncated protein and to haploinsufficiency (see http://lbbma.univ-angers.fr) (Ferre *et al.*, 2005). These mutations are invariably associated with a non-syndromic, slowly progressive form of optic neuropathy, as originally described by Kjer (1959). Classic DOA usually begins before 10 years of age, with a large variability in the severity of clinical expression, which may range from non-penetrant unaffected cases up to very severe, early onset cases, even within the same family carrying the same molecular defect (Delettre *et al.*, 2002; Carelli *et al.*, 2004; Olichon *et al.*, 2006; Cohn *et al.*, 2007). However, there is at least one clear example standing out of this paradigm. This is a mutation in the *OPA1* gene, i.e. the c.1334G>A leading to p.R445H amino acid change, being associated with a syndromic form of optic neuropathy and sensorineural deafness (Amati-Bonneau *et al.*, 2003; Shimizu *et al.*, 2003), and in some of the reported cases with chronic progressive external ophthalmoplegia (CPEO), ptosis and myopathy (Treft *et al.*, 1984; Meire *et al.*, 1985; Payne *et al.*, 2004).

CPEO, isolated or variably associated with a wider syndromic clinical expression, is the most frequent feature of mitochondrial myopathy and has a heterogeneous genetic basis, again driven by both primary defects in the mtDNA, i.e. single deletions and point mutations (DiMauro and Schon, 2003), or by mutations in nuclear genes resulting in multiple deletions of mtDNA (Zeviani *et al.*, 1989). At least four nuclear genes are now known to be involved in CPEO associated with mtDNA multiple deletions and autosomal recessive or dominant inheritance. These are *POLG1* (Van Goethem *et al.*, 2001), the enzyme replicating mtDNA, the mitochondrial replicative DNA helicase Twinkle (*PEO1*) (Spelbrink *et al.*, 2001), the heart/muscle-specific adenine nucleotide translocator ANT1 (*SLC25A4*) (Kaukonen *et al.*, 2000), and finally the thymidine phosphorylase (*TP*) involved in the nucleoside pool maintenance (Nishino *et al.*, 1999). Among these genes, mutations in at least two of them, i.e. *POLG1* and *TP*, may present with a combination of deletions and depletion of mtDNA in skeletal muscle (Hirano *et al.*, 2004; Hudson and Chinnery, 2006).

The association of CPEO and mitochondrial myopathy with optic atrophy is not frequent (Treft *et al.*, 1984; Meire *et al.*, 1985) and never reported as due to mutations in the above-mentioned genes. Thus, the clinical phenotype associated with the *OPA1*/R445H mutation is somehow a novel combination bridging autosomal-dominant CPEO and DOA (Payne *et al.*, 2004). Recent studies showed that the biochemical phenotype of the *OPA1*/R445H mutation consists in a defective OXPHOS in fibroblasts (Amati-Bonneau *et al.*, 2005). A defect in muscle bioenergetic efficiency was also documented by MR spectroscopy (MRS) in patients with the c.2708delTTAG microdeletion and classic DOA (Lodi *et al.*, 2004). Furthermore, slight reduction of mtDNA copy number was reported in blood cells from DOA patients (Kim *et al.*, 2005), overall supporting the notion that OPA1 may be involved in control of mtDNA content and ultimately in OXPHOS efficiency.

We here report the association of different mis-sense point mutations in the *OPA1* gene in six families affected with 'plus' phenotypes of optic atrophy and wider

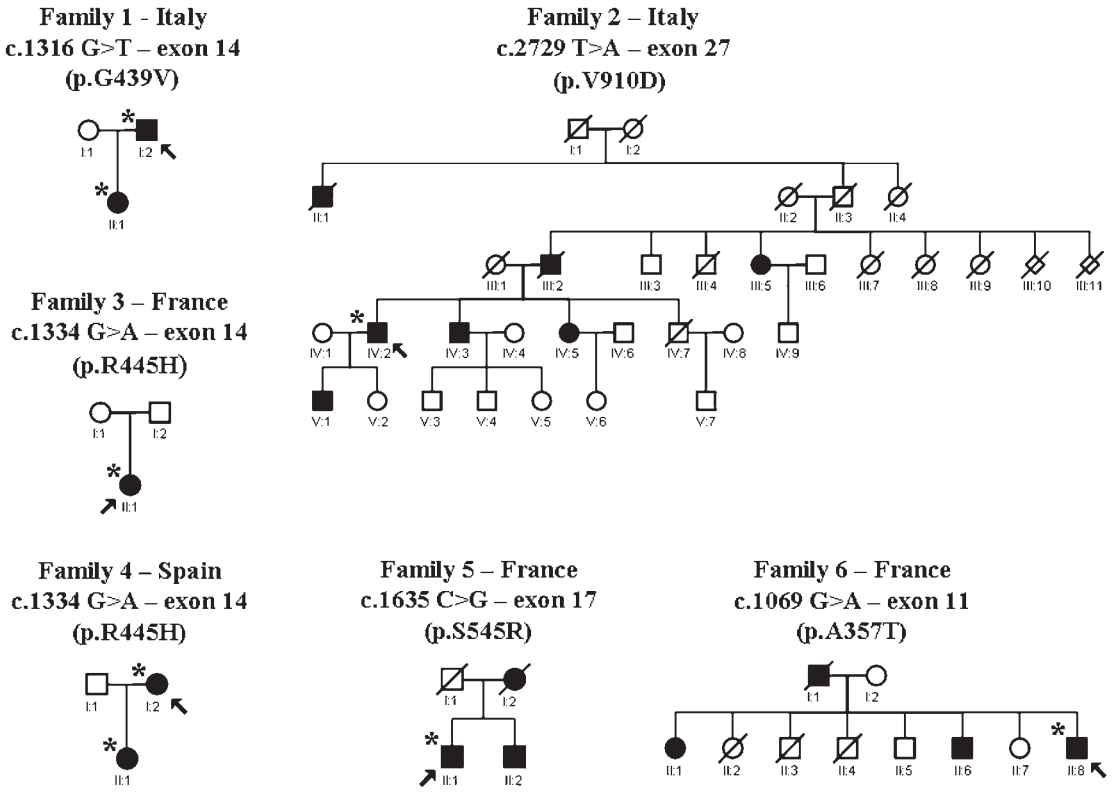

Fig. 1 Genealogical trees of the families investigated. Arrows indicate the probands of each pedigree, for which geographic origin and the OPA1 mis-sense point mutation, exon, and amino acid change are also provided. Asterisks indicate the individuals for which a clinical history has been provided in the text. With the exception of Family 3, which is a sporadic case with a *de novo* mutation, all the other families showed a pattern compatible with autosomal-dominant inheritance.

neuromuscular involvement including sensorineural deafness, cerebellar ataxia, axonal sensory-motor polyneuropathy and mitochondrial myopathy frequently complicated by CPEO. Most remarkably we provide evidence that multiple deletions of mtDNA are accumulated in the skeletal muscle of these patients, thus revealing an unrecognized role of the OPA1 protein in maintaining mtDNA integrity.

Patients and methods

Case reports

We here present the clinical histories of eight patients belonging to the six families investigated (Fig. 1) and a summary of the clinical and laboratory findings is reported in Table 1.

Case 1 (Family 1, 1-2)

This family is fully described elsewhere and we here detail again the clinical histories of the two affected subjects (Liguori *et al.*, in press). The proband is a 38-year-old man from Italy who was noted for poor vision at 4 years of age. At 6 years of age a rapid deterioration of his visual acuity led this patient to legal blindness. At 9 years of age he also suffered a progressive hearing loss needing acoustic prosthesis. At 30 years of age he developed gait difficulties with frequent falls. We observed this patient for the first time when he was 38 years old and his neurological exam showed bilateral ophthalmoplegia and optic atrophy, severe deafness, pes cavus, hypopallestesia at lower limbs, weak deep tendon reflexes, positive Romberg sign and ataxic gait. Laboratory investigations showed mild elevation of AST (45 U/l, normal value <38) and ALT (65 U/l, normal value <41). Serum lactic acid after standardized exercise was abnormally elevated (54.5 mg/dl, normal value <22). Muscle biopsy was positive for Ragged Red Fibres (RRFs) and cytochrome *c* oxidase (COX) negative fibres (Fig. 2, panels A, B and C). Electron microscopy of skeletal muscle showed mitochondria with morphologically abnormal cristae and accumulation of lipid droplets. Nerve conduction studies revealed a mild sensory-motor axonal neuropathy. Somatosensorial evoked potentials (SEPs) showed absent cortical responses from the lower limbs and increased latencies from the upper limbs, suggestive of a posterior column involvement. Motor evoked potentials (MEPs) were normal. Pattern visual evoked potentials (PVEPs) showed absent cortical responses bilaterally, whereas electroretinogram was unremarkable. Brainstem auditory evoked potentials (BAEPs) showed absent responses on left ear and increased latencies of the IV and V response with absence of II and III response on right ear. Audiometric exam showed a severe bilateral sensorineural hearing loss. A brain MRI showed variable degrees of atrophy affecting cerebral cortex, brainstem and cerebellum (Fig. 3, panel A). Bilateral hypointensity of basal ganglia was detected at the gradient echo MRI scan, which at CT scan was compatible with bilateral calcifications (Fig. 3, panels B and C). Electrocardiogram (EKG) was normal.

Table 1 Summary of clinical and laboratory findings

Family/Case/ Sex/Age	Optic atrophy	Ptosis/ CPEO	Deafness	Ataxia/ Romberg sign	Clinical myopathy	Peripheral (axonal) neuropathy at electrophysiology	Muscle Biopsy	mtDNA multiple deletions	Mitochondrial network in fibroblasts	OPA1 mutation
Family 1/Case 1/M/38	+	−/+	+	+/+	−	+	RRFs/COX -	+	Fragmented	c.1316 G>T (p.G439V)
Family 1/Case 2/F/7	+	−/−	+	−/−	−	−	NA	NA	NA	c.1316 G>T (p.G439V)
Family 2/Case 1/M/59	+	−/−	−	−/−	−	−	Non specific myopathic changes	+	NA	c.2729 T>A (p.V910D)
Family 3/Case 1/F/39	+	−/−	+	+/+	−	NA	RRFs/COX -	+	Fragmented (Amati-Bonneau *et al.*, 2005)	c.1334 G>A (p.R455H)
Family 4/Case 1/F/57	+	+/+	+	−/−	Exercise intolerance	+	RRFs/COX −	+	Fragmented (Amati-Bonneau *et al.*, 2005)	c.1334 G>A (p.R455H)
Family 4/Case 2/F/9	+	−/−	+	−/−	−	NA	NA	NA	Fragmented (Amati-Bonneau *et al.*, 2005)	c.1334 G>A(p.R455H)
Family 5/Case 1/M/43	+	+/+	+	+/+	Diffuse myalgia	+	RRFs/COX -	+	NA	c.1635 C>G (p.S545R)
Family 6/Case 1/M/67	+	+/+	+	−/−	Muscle weakness	+	RRFs/COX -	+	NA	c.1069 G>A (p.A357T)

M = male; F = female; CPEO = chronic progressive external ophthalmoplegia; RRFs = ragged red fibres; COX- = cytochrome *c* oxydase negative fibres; NA = not available.

Case 2 (Family 1, II-1)

This 7-year-old girl is the only daughter of the proband of Family 1, being born by caesarean delivery of non-consanguineous parents. She had initial feeding difficulties and a slight delay in her motor and language development. At 6 years of age she was noted to have difficulties in watching the television. At this time a marked pallor of the optic disc was reported and an audiometric exam revealed a sensorineural hearing loss. Cerebral MRI and CT scan were normal, as well as nerve conduction studies. We observed the patient when she was 7 years old and her neurological examination was essentially normal except for the optic atrophy and hearing loss. Basal serum lactic and pyruvic acid were normal. A new audiometric exam confirmed the sensorineural hearing loss. Electroencephalogram (EEG) and EKG were normal. Except for her father there are no other family members being affected by visual and hearing loss, nor other neurological symptoms.

Case 1 (Family 2, IV-2)

This 59-year-old proband belongs to an Italian family with at least other six affected individuals with autosomal-dominant transmission of optic atrophy. He has suffered a slowly progressive visual loss since childhood, initially prevalent on the right eye. We observed this patient when he was 57 years old and his neurological examination was remarkable only for bilateral optic atrophy and diffusely weak deep tendon reflexes. Serum lactic acid after standardized exercise was abnormally elevated (37.6 mg/dl, normal values <22). Muscle biopsy showed non-specific signs of myopathy (Fig. 2, panels D, E and F), but electron microscopy revealed paracristalline inclusions in mitochondria. Audiometric exam was essentially normal as well as BAEPs. PVEPs showed markedly reduced amplitudes and increased latencies of cortical responses. The electroretinogram was unremarkable. Ophthalmologic investigations showed reduced visual acuity (2/10 OD, 6/10 OS), pale optic discs at fundus and a central scotoma at visual field exam.

Case 1 (Family 3, II-1)

The case of this 39-year-old French woman has already been reported (Amati-Bonneau *et al.*, 2003, 2005) but at that time we had no information on the muscular pathology. Briefly, she presented with optic atrophy at the age of 6 years and with moderate sensorineural hearing impairment since the age of 15 years. Neurophysiological studies (BAEPs and evoked otoacustic emissions) suggested that deafness was caused by auditive neuropathy. At a recent neurological examination she showed severe optic atrophy and deafness and mild ataxia with positive Romberg sign. She underwent muscle biopsy that showed evidence of RRFs and COX negative fibres (Fig. 2, panels G, H and I).

Case 1 (Family 4, I-2)

This patient and her daughter were also previously reported (Amati-Bonneau *et al.*, 2005). Briefly she is a 57-year-old Spanish woman who has been diagnosed with optic atrophy at age 13 years and a moderate sensorineural hearing loss was found when she was 30 years old. The first audiogram at 33 years of age showed a predominant high-frequency hearing loss, and she displayed a progressive worsening of auditory function over the following years. At age 56 years, she complained of exercise intolerance and

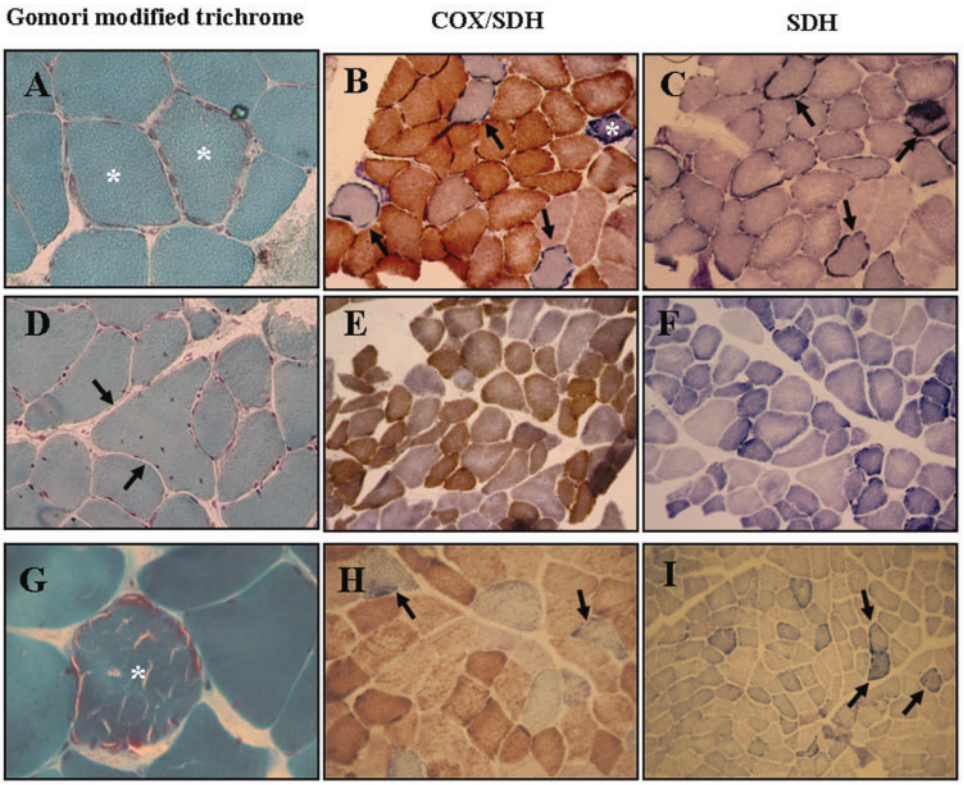

Fig. 2 Muscle histopathology (Gomori modified trichrome, COX/SDH and SDH stain). (**A**), (**B**) and (**C**) refer to the proband of Family I. In panel A two fibres displaying increased eosinofilic material with subsarcolemmal distribution, which resemble RRFs are shown (asterisks). In panel B, at the double COX/SDH stain some COX-deficient fibres are recognized by the prevalent SDH violet stain (arrows), and one hyperintense SDH fibre is also shown (asterisk). In panel C, a section serial to the previous in panel B shows numerous fibres with increased SDH stain, in particular in the subsarcolemmal region (arrows). (**D**), (**E**) and (**F**) refer to the proband of Family 2. In panel D a hypertrophic fibre is shown with numerous centralized nuclei (arrows), whereas this patient did not present RRFs. Panels E and F also show the great variability of fibre size, but no clear COX-deficient or hyperintense SDH fibres were present. However, a prevalent SDH stain was frequent in some fibres at COX/SDH double stain, as well as some parcellar increase of SDH only stain was evident in a few fibres. (**G**), (**H**) and (**I**) refer to the proband of Family 3. In panel G a typical RRFs is shown (asterisk). In panel H frequent COX-deficient fibres are seen (arrows), and in panel I increased subsarcolemmal staining of SDH is present in numerous fibres (arrows).

EMG documented both myopathy and peripheral neuropathy. She underwent muscle biopsy, which revealed RRFs and COX negative fibres. Muscle respiratory chain enzyme activities were essentially normal, even if on the low side of the control range (data not shown). She now suffers of bilateral ptosis and ophthalmoplegia, hypotiroidism, dysphagia and slight cognitive impairment.

Case 2 (Family 4, II-1)

The daughter of the proband of Family 4 was also diagnosed with optic atrophy and hearing loss at age 9 years. Her clinical condition is now slowly progressing.

Case 1 (Family 5, II-1)

This 43-year-old man from southern France suffered visual impairment since childhood and diffuse myalgia in both legs since adolescence. At age 39 years he experienced gait difficulties and ataxia was reported at neurological examination. At age 42 years, he was admitted to a gastroenterology unit for an episode of colic occlusion without any evident mechanical cause and was thereafter admitted in the neurology unit. At this time, his visual acuity was reduced to counting fingers in both eyes and fundus examination showed bilateral optic atrophy. At neurological examination he also had bilateral ptosis and ophthalmoplegia, impaired sensation to all modalities predominantly in the lower limbs, marked gait ataxia and positive Romberg sign. Neurophysiological studies (BAEPs and evoked otoacustic emissions) showed auditive neuropathy. EMG revealed an axonal sensory-motor neuropathy without clear evidence of myopathy. Muscular biopsy evidenced RRFs and COX negative fibres. Brain MRI revealed an atrophy of the corpus callosum and brainstem and a mild cerebellar atrophy (Fig. 3, panel D). Furthermore, bilateral basal ganglia hypointensity was detected at T2-weighted MRI scan (Fig. 3, panels E and F). Interestingly, brain MRS was normal, notably the lactate content (data not shown). The family history of this proband was remarkable for optic atrophy in his mother and brother, but we did not obtain further details from these cases.

Case 1 (Family 6, II-8)

This 67-year-old man from western France had bilateral ptosis and moderate hearing loss since childhood. At age 60 years, he developed bilateral cataract requiring surgery. At age 67 years, he was admitted in a neurological unit complaining muscular weakness. At neurological examination he had bilateral ptosis

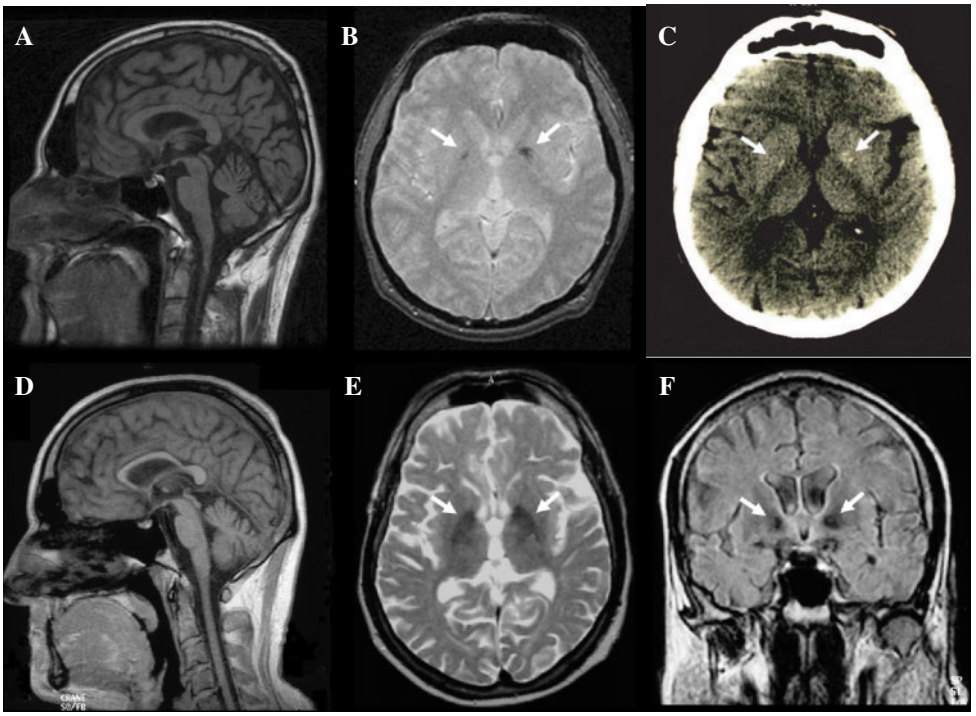

Fig. 3 Brain MRI and CT scan. (**A**), (**B**) and (**C**) refer to the proband from Family I. In panel A a mid-sagittal T1-weighted brain MRI scan shows variable degrees of atrophy affecting cerebral cortex, brainstem and cerebellum. In panel B the axial gradient echo MRI scan shows bilateral hypointensity within the globi pallidi (arrows), which is detected as depositions of calcium in the CT scan (arrows) shown in panel C. (**D**), (**E**) and (**F**) refer to the proband from Family 5. In panel D a mid-sagittal T1-weighted brain MRI scan shows a thin corpus callosum as well as brainstem and cerebellar atrophy. In panel E the axial T2-weighted scan shows bilateral hypointensity within the globi pallidi, which are also detected in the coronal scan (arrows) shown in panel F.

and ophthalmoplegia, mild optic atrophy and areflexia at four limbs. Muscular CPK as well as blood and CSF lactate levels were normal. EMG revealed an axonal sensory-motor neuropathy and myopathic involvement of orbicularis oculi muscle. Muscular biopsy evidenced numerous RRFs and COX negative fibres and electron microscopy revealed paracristalline inclusions in mitochondria. The family history of this patient was remarkable for ptosis in his father, sister and brother but no further clinical details were available on these patients.

Muscle histopathology and ultrastructure

Quadriceps, deltoid, or tibialis anterior muscle biopsies, either by needle or open surgery, were performed under local anaesthesia and after informed consent of the patient. Muscle specimens were frozen in cooled isopentane and stored in liquid nitrogen for histological and histoenzymatic analysis including Gomori modified trichrome staining, COX activity, succinate dehydrogenase (SDH) activity and double COX/SDH staining according to standard protocols. A fragment was also fixed in 2% glutaraldehyde and processed for ultrastructural analysis.

Fibroblasts culture

Fibroblasts culture was established from skin biopsies, having obtained informed consent of the patient. Fibroblasts were grown in DMEM medium supplemented with 10% fetal bovine serum (FBS), 2 mM l-glutamine and antibiotics. For the experiments, fibroblasts were grown in DMEM glucose medium or DMEM glucose-free medium containing 5 mM galactose, 5 mM pyruvate (DMEM galactose medium). Mitochondrial morphology was assessed after cell staining with 10 nM Mitotracker (Molecular Probes) for 30 min at 37°C. Fluorescence was visualized with a digital imaging system using an inverted epifluorescence microscope with 63×/1.4 oil objective (Diaphot, Nikon, Japan). Images were captured with a back-illuminated Photometrics Cascade CCD camera system (Roper Scientific, Tucson, AZ, USA) and Metamorph acquisition/analysis software (Universal Imaging Corp., Downingtown, PA, USA).

Molecular investigations

Informed consent for genetic investigations was obtained from all patients after approval of the study by the board of the local ethical committee in the different institutions participating to this project. Total DNA was extracted from the platelet/lymphocyte fraction and skeletal muscle by the standard phenol/chloroform method.

Sequencing of the OPA1 gene

For the *OPA1* gene analysis genomic DNA was amplified by PCR with specific primers designed to amplify all exons and flanking intronic regions as previously described (Pesch *et al.*, 2001). PCR reactions were carried out in a 50 µl volume with 50–100 ng genomic DNA, 10 mM Tris–HCL pH 8.9, 50 mM KCL, 1,5-3 mM $MgCl_2$ and 200 µM of each dNTP, 10 pmol of primers and 1 U AmpliTaq polymerase (Applied Biosystems, Weiterstadt, Germany).

PCR products were purified by ExoSAP treatment (Amersham) and sequenced employing BigDye Terminator chemistry (Applied Biosystems).

Analysis of mtDNA deletions

Southern blot analysis was performed, as previously reported (Moraes *et al.*, 1989), on the linearized mtDNA molecule after digestion with the restriction enzyme *Pvu*II, separated by agarose electrophoresis (0.8%), transferred onto nitrocellulose membranes and hybridized with the entire human mtDNA probe labelled with digoxigenin-alkaline phosphatase (Roche Diagnostics, Switzerland).

Long-range PCR on mtDNA was also performed by two different protocols. One method is essentially as reported by Nishigaki *et al.* (2004). The set of primers used is as follows: F1482-1516 and R1180-1146 (wild-type mtDNA fragment of 16.267 bp) F3485-3519 and R14820-14786 (wild-type mtDNA fragment of 11.335 bp), F5459-5493 and R735-701 (wild-type mtDNA fragment of 11.845 bp). The PCR conditions were: one cycle at 94°C for 1 min; 30 cycles at 98°C for 10 s and 68°C for 11 min; a final superextension cycle at 72°C for 10 min. The PCR was performed using Takara LA Taq DNA polymerase for the first pair of primers, and Takara Ex Taq DNA polymerase for the other set of primers (Takara Shuzo Corp., Japan). The PCR products were separated by a 0.8% agarose gel. The second method is just similar to the one previously described, the PCR being performed by using Takara LA Taq DNA polymerase (Takara Shuzo Corp., Japan) and two set of primers: F8285-8314 and R15600-15574 (wild-type mtDNA fragment of 7315 bp); F8285-8314 and R13705-13677 (wild-type mtDNA fragment of 5420 bp). The PCR conditions were one cycle at 94°C for 2 min; 30 cycles at 98°C for 5 s and 68°C for 15 min; a final superextension cycle at 72°C for 10 min.

Sequencing of mtDNA

The complete mtDNA was amplified in 24 overlapping PCR fragments using specifically designed primers (available upon request) based on the revised human mtDNA Cambridge reference sequence (www.mitomap.org/mitoseq.html) (Andrews *et al.*, 1999). The PCR fragments were sequenced in both directions using a dye terminator cycle sequencing kit (Applera, Rockville, MD). Assembling and identification of variations in the mtDNA was carried out using the Staden Package (Staden *et al.*, 2000).

Sequencing across the junction points of some mtDNA deletions was achieved by amplifying specific mtDNA fragments to detect the 5 kb deletion, using the set of primer F8287-8306 and R13590-13571, and the 8.1 and 7.6 kb deletion using the set of primer F5651-5670 and R14268-14249. The PCR conditions were: one first cycle at 94°C for 5 min; 30 cycles at 94°C for 1 min, 55°C for 1 min, 72°C for 1 min; a final superextension cycle at 72°C for 7 min. The PCR products, isolated from the agarose gels by QIAquick gel extraction kit (Qiagen, Valencia, CA), were sequenced in an ABI Prism 310 Genetic Analyzer using Big Dye Terminator Cycle Sequencing Reaction Kits (Applied Biosystems).

Evaluation of mtDNA copy number

Quantitation of mtDNA relative to nuclear DNA (nDNA) was performed by two real-time PCR-based different methods. Both were multiplex assays based on hydrolysis probe chemistry. In the first method the target genes were the 12S ribosomal gene of mtDNA (primers and probe sequences and PCR reaction conditions are available on request) and the RNAseP nuclear gene (TaqMan RNAseP Control Reagent Kit, Applied Biosystems, Foster City, CA, USA). Calibration curves were used to quantify mtDNA and nDNA copy number, which were based on the linear relationship between the crossing points cycle values and the logarithm of the starting copy number.

The second method was as previously described (Cossarizza *et al.*, 2003). Briefly, a mtDNA fragment (nt 4625-4714) and a nuclear DNA fragment (*FasL* gene) were co-amplified by multiplex polymerase chain reaction. PCR reaction conditions, primers and probes are as previously detailed (Cossarizza *et al.*, 2003). A standard curve for mtDNA and nuclear DNA was generated using serial known dilutions of a vector (provided by Genemore, Modena, Italy) in which the regions used as template for the two amplifications were cloned tail to tail, to have a ratio of 1:1 of the reference molecules.

For both methods the data are means of at least three independent measurements.

Sequencing of nuclear genes involved in mtDNA multiple deletions

Direct sequencing of the complete coding region and the exon/intron boundaries of the genes *POLG1*, *PEO1* (Twinkle) and *SLC25A4* (ANT1) were carried out as previously described (Gonzàlez-Vioque *et al.*, 2006) in an ABI 3730 (Applied Biosystems, Foster City, CA, USA) sequencer.

OPA1 protein homology modelling

The OPA1 sequence (gi:18860834;NM_130833.1), was submitted to profile–profile sequence searches with the FFAS (Jaroszewski *et al.*, 2002) server (http://ffas.ljcrf.edu). Bacterial dynamin like protein (BDLP GI:122920796) was identified as the most significant hit (*FFAS score -44.1)* with a sequence identity of 13% in the region of 220-940 of OPA1. The BDLP coordinates (*PDB-ID 2j68)* (Low and Lowe, 2006) were used as a template for modelling the OPA1 structure with the SCWRL-Server (http://www1.jcsg.org/scripts/prod/scwrl) using default settings with conformations of conserved residues retained. Manual inspection, mutagenesis and figures were done using program PyMOL (DeLano Scientific).

Statistics

Data were analysed by one-way ANOVA, using the software SigmaStat Ver. 3.5 (Systat Software Inc.). Data were considered significantly different when P-values <0.05.

Results

Mutation analysis of *OPA1* gene

All six probands with optic atrophy 'plus' clinical phenotypes underwent complete sequence analysis of the *OPA1* gene and in each case a mis-sense pathogenic mutation was found. Sequencing of the mutated exon was performed in other members of the family, when available, and revealed a full penetrance of the mutated alleles in

other affected patients. The mutation c.1316 G>T (p.G439V) in exon 14, found in Family 1, was previously reported and molecular analysis of multiple family members demonstrated that the mutation was present only in the proband and her daughter suggesting a *de novo* event (Liguori *et al*., in press). The mutation of Family 1 is close to the previously reported mutation c.1334 G>A (p.R445H) in exon 14 (Treft *et al*., 1984; Meire *et al*., 1985; Shimizu *et al*., 2003; Amati-Bonneau *et al*., 2003; Payne *et al*., 2004), which was found in Family 3 and Family 4 of our series. Both these mutations, as well as the others identified in Family 5 (c.1635 C>G, p.S545R, exon 17) and Family 6 (c.1069 G>A, p.A357T, exon 11), introduce amino-acid changes in highly conserved positions of the GTPase domain and were not found in a panel of 460 control chromosomes. The mutation found in Family 5, which is of French ancestry, has also been detected in an unrelated pedigree from the United Kingdom displaying a similar clinical phenotype (Hudson *et al*, in this issue). Furthermore, this same mutation has also been previously found in a study on a series of DOA patients from Japan (Nakamura *et al*., 2006). Finally, the c.2729 T>A (p.V910D) mutation in exon 27 found in Family 2, stands out because it affects the GTPase effector domain and is associated with a milder phenotype compared to all other mutations (Table 1).

Muscle histochemistry and ultrastructure

All probands from the six families here reported underwent skeletal muscle biopsy and in all occasions, except for case 1 from Family 2, RRFs and/or COX negative fibres were detected at Gomori-modified trichrome and double COX/SDH staining (Table 1 and Fig. 2, panels A, B, G and H). SDH staining also showed different degrees of mitochondrial proliferation ranging from increased subsarcolemmal staining to full SDH positive fibres (Fig. 2, panels C and I). Case 1 from Family 2 again stands out because he did not display any clear sign of mitochondrial dysfunction at muscle histochemistry, even if a frequent prevalence of the SDH stain was observed at double COX/SDH staining, possibly indicative of a partially depleted COX activity (Fig. 2, panel E). However, this patient had non-specific histological changes, such as marked variability of fibres size with both hypo and hypertrophic changes, splitting fibres, central nuclei and sporadic subsarcolemmal rimmed vacuoles, all suggestive of myopathy (Fig. 2, panels D and F). He underwent muscle biopsy because of pathological serum lactate levels after standardized muscle exercise (see case report). Overall, the patients of our case series ranged between age 38 and 67 years and, with the exception of case 1 from Family 2, RRF were 2.5 to 8%, SDH hyperintense fibres were 6 to 35%, and finally COX negative fibres were 7 to 35%. In all cases who underwent electron microscopy there was ultrastructural evidence of mitochondrial pathology, including the proband from Family 2, most frequently mitochondrial proliferation, altered morphology of mitochondria and cristae organization, and paracristalline inclusions (Fig. 4).

Fig. 4 Ultrastructure of skeletal muscle. At electron microscopy, a collection of aberrant subsarcolemmal mitochondria is recognizable, with 'parking lot'-like paracristallin inclusions, in the muscle biopsy from the proband of Family 6.

Mitochondrial DNA analysis

The finding of clear signs of mitochondrial myopathy, with a mosaic distribution of RRFs and COX negative/SDH hyperintense fibres pointed to the possible occurrence of mtDNA defects and prompted various molecular investigations on mtDNA. Initially, due to the apparent maternal inheritance, the index case of Family 4 underwent a complete sequence analysis of muscle mtDNA, which did not reveal any candidate pathogenic mutation. All changes detected were well established population-specific polymorphic variants defining haplogroup J1 and the complete sequence has been deposited in GenBank [http://www.ncbi.nlm.nih.gov/Genbank/GenbankOverview.html (accession number is EU151466)]. None of the other probands underwent complete mtDNA sequence analysis, mostly because of unequivocal evidence of dominant transmission of the disease, as in Families 1, 2 and 6.

All probands underwent mtDNA analysis to screen for the presence of large-scale rearrangements, either by Southern blot analysis followed by long PCR, or directly by long-range PCR when the availability of muscle mtDNA was limited. All probands who underwent Southern blot analysis (Families 3, 4, 5 and 6) showed variable levels of mtDNA multiple deletions (one example is given in Fig. 5, panel A). The presence of multiple deletions was confirmed in all probands by long-range PCR performed with different sets of primers (Fig. 5, panels B and C). We did not perform quantitative analysis, but the abundance of multiple deletions was quite variable ranging from patients with very low levels (Fig. 5, line 1 in panel C) to cases with

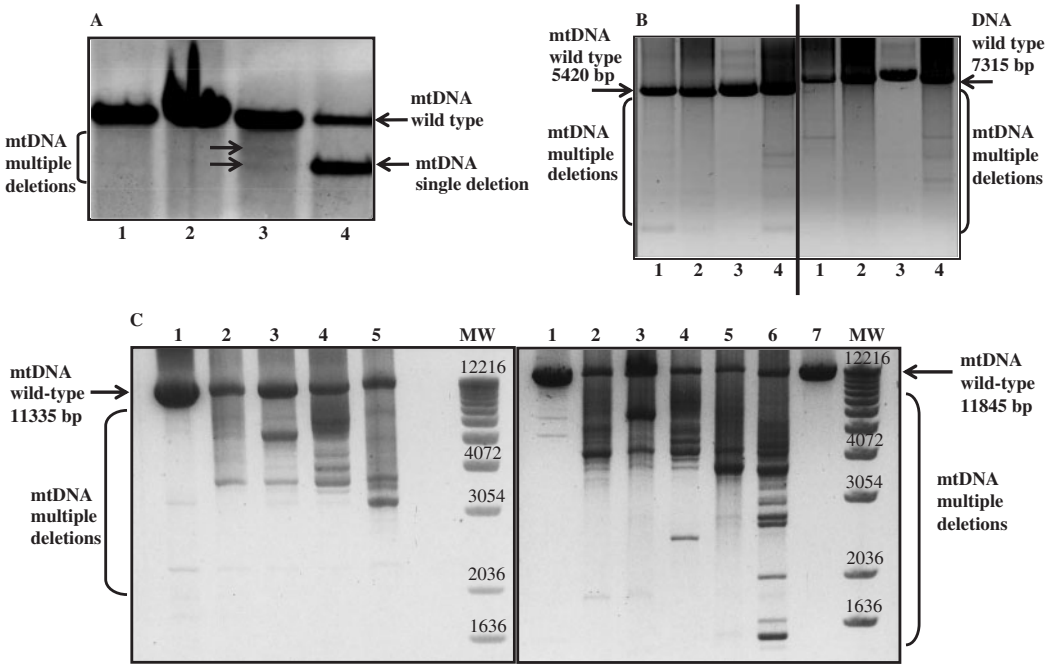

Fig. 5 Molecular investigation. (**A**) Southern blot analysis (proband from Family 4). Lanes 1 and 2 are muscle DNAs from two age-matched healthy controls, who show the presence of a single band correspondent to wild-type mtDNA. Lane 3 is muscle DNA from the proband of Family 4, showing multiple bands: the wild-type mtDNA and at least other two lighter bands of very low intensity corresponding to deleted mtDNA molecules. Lane 4 is muscle DNA from a patient with a single large-scale mtDNA deletion. Arrows indicated mtDNA deleted molecules. (**B**) Long PCR (proband from Family 4). This panel shows an agarose electrophoresis separation of the wild-type mtDNA long-PCR amplified fragment of 5420 bp on the left, and the fragment of 7315 bp on the right (see 'Methods' section for details). Lane 1 shows wild-type and deleted molecules of muscle mtDNA from a patient known to carry mtDNA multiple deletions as detected by Southern-blot (positive control); Lane 2 shows a single wild-type mtDNA band amplified from muscle DNA of a healthy individual (negative control); Lane 3 shows a single wild-type mtDNA band amplified from fibroblast DNA of the proband from Family 4; Lane 4 shows wild-type and deleted molecules in the muscle mtDNA of the proband from Family 4. (**C**) Long PCR (probands from all other families). This panel shows an agarose electrophoresis separation of the wild-type mtDNA long-PCR amplified fragment of 11.335 bp on the left, and the fragment of 11.845 bp on the right (see 'Methods' section for details). Variably abundant extrabands due to mtDNA deleted molecules from muscle DNA of all probands except the one from Family 4 are present. Lane 1 is proband from Family 2; Lane 2 is proband from Family 1, Lane 3 is proband from Family 5, Lane 4 is proband from Family 3, Lane 5 is proband from Family 6 in both left and right electrophoresis; in the right electrophoresis Lane 6 is a positive control (a CPEO patient previously diagnosed with mtDNA multiple deletions) and Lane 7 is a negative control. Molecular weight is marker X (Roche) and the size of some reference bands is indicated. The presence of mtDNA deletions in all these probands has been further confirmed using the other set of primers described in the methods (not shown).

higher abundance (Fig. 5, line 4 in panel C). To confirm that the bands detected by long-range PCR were truly deleted molecules of mtDNA, we specifically re-amplified by PCR with appropriate primers some of the putative deletions, purified the band and performed sequence analysis detecting the junction point of the deleted molecule (Fig. 6). The proband from Family 4 was not investigated by this approach, because muscle DNA was no longer available. We detected the ΔmtDNA 4.9 kbp (common deletion) in all the other probands investigated (the same of panel C in Fig. 5).The ΔmtDNA 8.1 kbp was particularly abundant in proband 1 from Family 2, but present only at low level in all other cases, whereas the ΔmtDNA 7.6 kbp was easily detected in all probands except the one from Family 2.

The absolute quantitation of mtDNA copy number was performed on DNA samples extracted from skeletal muscle of the six probands and of 14 normal individuals (Fig. 7). As negative and positive controls we respectively used total DNA extracted from 143B.TK-derived 209 Rho 0 cells (a kind gift of Giuseppe Attardi), completely devoid of mtDNA, and from skeletal muscle of a patient with mitochondrial encephalomyopathy, lactic acidosis and stroke-like (MELAS) syndrome with abundant RRFs and over 80% heteroplasmy of the 3243A>G $tRNA^{Leu}$ mtDNA point mutation (Valerio Carelli, data not shown).

The mean values of mtDNA copy number in control groups were 1949 ± 948 (age-matched controls) and 2008 ± 927 (total controls). We found similar values in affected individuals, except for the probands of Families 3 and 6 that showed a non-significant increase of mtDNA copy number compared to the control group, respectively 3185 ± 1431 and 2954 ± 1033 (Fig. 7).

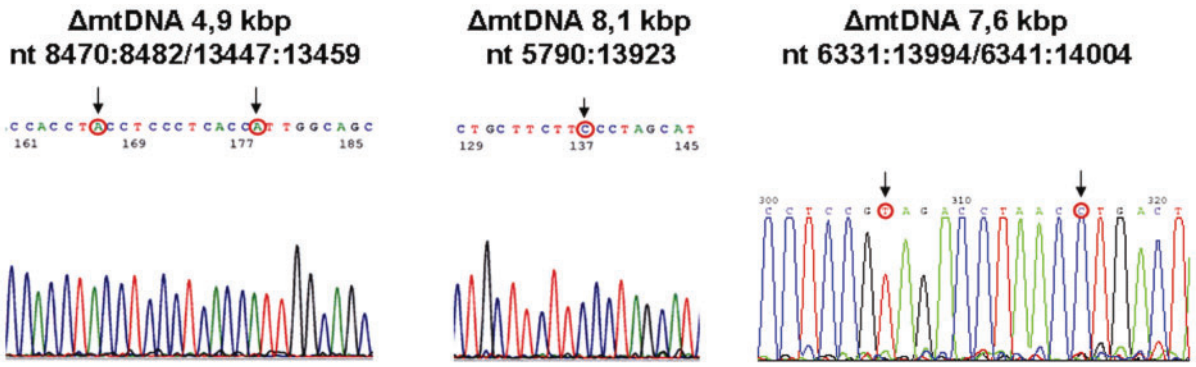

Fig. 6 ΔmtDNA junction points. The deletion junctions of three different mtDNA deletions (4.9 kbp or common deletion in the proband from Family 1; 8.1 kbp in the proband from Family 2; 7.6 kbp in the proband from Family 5) amplified from muscle DNA and directly sequenced are shown. The arrows on the sequence pherograms delimitate the repeat location at the boundaries of each mtDNA deletion and corresponding nucleotide positions are also indicated.

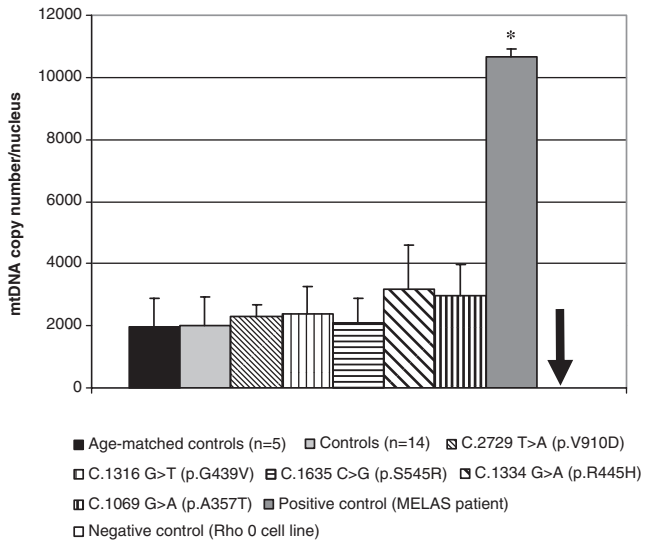

Fig. 7 mtDNA content assay. The assessment of muscle mtDNA copy number of OPA1 patients is shown in comparison with normal controls (age-matched and not) and with positive (a patient with MELAS syndrome with abundant RRFs) and negative (143B.TK- derived 209 Rho 0 cells; arrow) controls. *Represents a *P*-value <0.05, the arrow indicates the negative control.

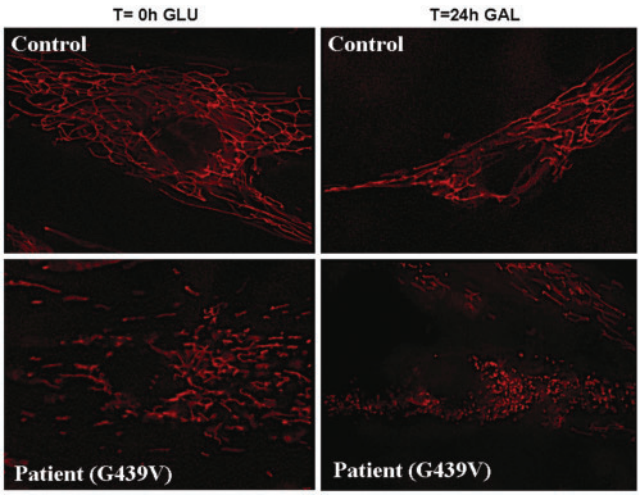

Fig. 8 Mitochondrial network in fibroblasts. The mitochondrial network of fibroblasts, as visualized by the Mitotracker Red dye, is shown comparing a control subject with the proband from Family 1 at time 0 in glucose medium, and after 24 h growth in galactose medium. The two conditions do not influence the interconnected tubular organization of the filamentous mitochondrial network in the control fibroblasts. The patient's fibroblasts present less interconnected filamentous mitochondria in glucose medium and after 24 h growth in galactose medium the mitochondrial network is completely fragmented.

Mitochondrial network in fibroblasts

Considering that OPA1 function is thought to be relevant for mitochondrial network organization, we investigated the mitochondrial morphology of fibroblasts bearing the *OPA1* mis-sense mutation c.1316 G>T (p.G439V) in exon 14 (proband from Family 1) (Liguori *et al.*, in press) compared with fibroblasts obtained from normal individuals, in glucose medium and after 24 h incubation in glucose-free medium containing galactose. Under this latter condition cells are forced to rely predominantly on oxidative phosphorylation for ATP synthesis, given the low efficiency of this carbon source to feed the glycolytic pathway (Ghelli *et al.*, 2003). After loading with Mitotracker Red and examination by fluorescence microscopy, fibroblasts from control subjects displayed a typical filamentous interconnected network in both growth conditions, with glucose medium and after 24 h switch on galactose medium (Fig. 8). The OPA1 mutant fibroblasts presented with filamentous mitochondria, but less interconnected and occasionally with balloon-like enlargements, in glucose medium (Fig. 8). After 24 h growth in galactose medium the mitochondrial network of most OPA1 mutant fibroblasts underwent a complete fragmentation resulting in only non-interconnected discrete organelles (Fig. 8).

Fibroblast cells from Families 3 and 4 patients (Table 1) were previously investigated and shown to display similar propensity to hyperfragmentation of mitochondrial network (Amati-Bonneau *et al.*, 2005).

Exclusion of nuclear genes involved in mtDNA multiple deletions

To rule out the contribution of the genes known to be involved in mtDNA multiple deletion formation we performed their sequence analysis. No sequence changes of pathogenic significance were identified in the coding regions and flanking exon–intron boundaries for *POLG1*, *PEO1* and *SLC25A4*, excluding any involvement of these genes in the pathogenic mechanisms.

OPA1 protein modelling

Sequence searches indicate that OPA1 is a 961 amino acid residue protein belonging to a family of highly conserved GTPases related to Dynamin and the closest structural homologue identified to date is the bacterial dynamin-like protein (BDLP) (Low and Lowe, 2006). The BDLP structure provides an OPA1 homology model for the C terminal region of the transmembrane helix and the PARL cleavage site (residues 220–960). Currently, OPA1 is considered a mechano-enzyme that uses GTP hydrolysis to switch between distinct conformations implicated in membrane fusion. Except one, all *OPA1* mis-sense mutations found in the DOA patients here investigated reside in the highly conserved GTPase domain (Fig. 9). GTPase activity is critical for OPA1 function and these miss-sense mutations (A357T, G439V, R445H, S545R) affect the GTPase domain just adjacent to its active site potentially impairing GTP hydrolysis by locking the protein in an 'on' or 'off' state. Thus, these mutations may interfere with nucleotide binding and alter the affinity and hydrolysis rate of the GTPase domain. Overall, these mutations possibly impair the fine tuned conformational states of the active–inactive balance of OPA1, directly impacting on its properties. The only mis-sense mutation differently located (V910D) resides outside the GTPase domain, at the interface of the two effector domains performing the conformational change (Fig. 9). This mutation replaces a hydrophobic valine with a negatively charged aspartate and may impact the integrity of the interface by destabilizing the 'off' state leading to an activated conformation of the protein.

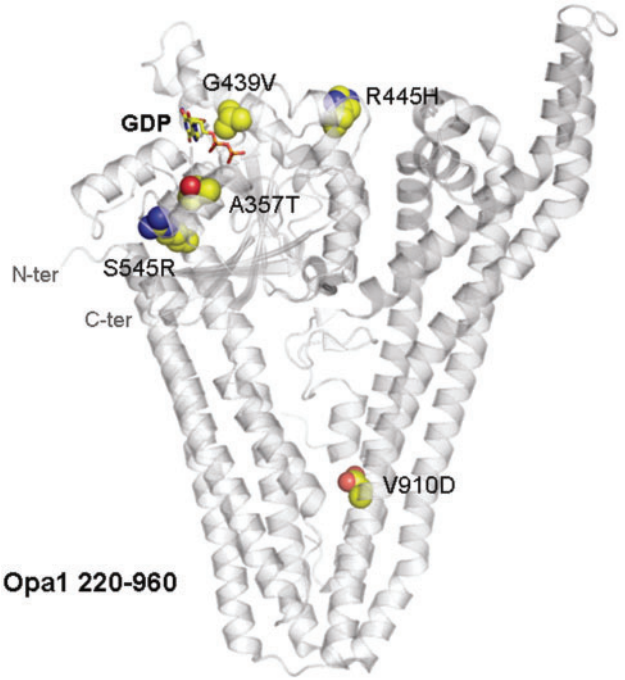

Fig. 9 OPA1 model and DOA mutations. Homology model of human OPA1 (gi|8860834|ref|NM_130833.1)), residues 220–960, based on the crystal structure of bacterial dynamin like protein (PDB-ID 2j68 (Low and Lowe, 2006), FFAS (Jaroszewski *et al.*, 2002) score -44.1, sequence identity 13%). OPA1 is shown as a grey cartoon with the GDP molecule bound to the GTPase domain depicted in sticks. The DOA mutations A357T, G439V, R445H, S545R and V910D are depicted in sphere mode with carbon atoms in yellow.

Discussion

In this study we show the unprecedented finding that mutations in the OPA1 gene, not predicted to produce protein truncation and haploinsufficiency as patho-mechanism for DOA, are associated with mtDNA instability and result in complicated clinical phenotypes that we propose to define as OPA1 'plus' syndromes. These clinical phenotypes seem to be invariably defined at least by the association of optic atrophy and muscular involvement, which may range from non-specific myopathy to classical mitochondrial myopathy with RRFs and COX negative fibres and CPEO, and in all cases except for Family 2 also by the occurrence of sensorineural deafness. Central and peripheral nervous system may also be variably involved, with frequent occurrence of cerebellar or spinocerebellar ataxia and peripheral axonal neuropathy. The common molecular feature we have found in all cases is the accumulation of multiple mtDNA deletions in the skeletal muscle from these patients. The age of the patients we have investigated ranged between 38 and 67 years, thus excluding that the amount of RRF/COX negative fibres and the levels of mtDNA multiple deletions we observed could be ascribed to their age-related somatic accumulation (Johnston *et al.*, 1995; Bua *et al.*, 2006). Our findings link for the first time OPA1 protein function with mtDNA integrity maintenance, making OPA1 the fifth gene involved in mtDNA multiple deletion pathologies, together with *POLG1*, *PEO1* (Twinkle), *SLC25A4* (ANT1) and *TP*.

OPA1 is a 960 amino acid residue protein that belongs to a family of highly conserved GTPases related to Dynamin (Praefcke and McMahon, 2004; Hoppins *et al.*, 2007). OPA1 is anchored to the mitochondrial inner membrane and has an important role in the mitochondrial fusion

process and in protection from apoptosis. Indeed, down-regulation of OPA1 using specific small interference RNA leads to fragmentation of the mitochondrial network concomitantly to dissipation of the mitochondrial membrane potential and to a drastic disorganization of the cristae (Olichon *et al.*, 2003). Moreover, OPA1 is also involved in protection from and regulation of the apoptotic process, by dealing with cytochrome *c* storage and release (Olichon *et al.*, 2003; Frezza *et al.*, 2006). Recent studies point to a mounting evidence that OPA1 is also involved in OXPHOS efficiency (Lodi *et al.*, 2004; Amati-Bonneau *et al.*, 2005), even if details of its mechanism and role in mitochondrial respiratory functions are lacking. One possibility is the involvement of OPA1 in regulating the amount of mtDNA, as suggested by a study showing that DOA patients may have slightly reduced mtDNA copy number in blood lymphocytes (Kim *et al.*, 2005). It is also known that mutant Mgm1 protein, the homologous protein of OPA1 in yeast, may lead to loss of mtDNA and *petit* phenotype (Herlan *et al.*, 2003). However, our current results on the possible involvement of OPA1 also in mtDNA maintenance in human subjects failed to reveal mtDNA depletion in the skeletal muscle of our probands, besides the documented occurrence of mtDNA instability with multiple deletions. On the contrary, in two cases the mtDNA copy number was increased compared with controls, even if without reaching statistical significance, in accordance with the presence of RRFs and compensatory enhancement of mitochondrial biogenesis.

It is remarkable that, contrary to the majority of the OPA1 mutations associated with DOA to date, all the mutations investigated in the present study are mis-sense point mutations changing amino acid residues in the highly conserved GTPase domain, with only one exception (V910D). This rules out haploinsufficiency as a patho-mechanism in our cases, and suggests more likely that gain or loss of function of the protein activity is responsible for mtDNA instability. The current hypothesis states that OPA1 is a mechano-enzyme that uses GTP hydrolysis to switch between distinct conformations that either facilitate membrane fusion directly or recruit machinery for it (Praefcke and McMahon, 2004; Olichon *et al.*, 2006; Hoppins *et al.*, 2007). GTPase activity is critical for OPA1 function and DOA miss-sense mutations found in the GTPase domain adjacent to its active site (A357T, G439V, R445H, S545R) may impair GTP hydrolysis locking the protein in an 'on' or 'off' state. Thus, these mutations have the potential to interfere with nucleotide binding and affinity, possibly affecting the hydrolysis rate of the GTPase domain. Hence, these mutations may alter the finely tuned conformational states of the active–inactive balance of OPA1 protein and have a direct impact on its properties. The other DOA miss-sense mutation, i.e. V910D in the GTPase effector domain, points to the existence of further such critical residues in the OPA1 protein. Knowing the possible involvement of dNTP pools in the mtDNA deletion formation in TP (Nishino *et al.*, 1999), and possibly in ANT1 (Kaukonen *et al.*, 2000) related syndromes, a scenario we may hypothesize, based on the currently reported OPA1 defects, is that differences in GTPase activity of OPA1 may affect the dGTP pool, ultimately leading to mtDNA instability.

However, OPA1 is attached to the inner mitochondrial membrane pointing towards the intermembrane space with a crucial, well-established role in cristae conformation (Olichon *et al.*, 2003, 2006; Frezza *et al.*, 2006). mtDNA nucleoids (Malka *et al.*, 2006) are also anchored to the same inner mitochondrial membrane but on the matrix side. Thus, the other possible mechanism through which OPA1 mis-sense mutations may lead to mtDNA instability is either the indirect interaction through changes in cristae morphology or the direct interaction of OPA1 protein through its N-terminal matrix-tail with mtDNA nucleoids and its possible role in stabilizing them. It is reasonable to predict that shifting the mitochondrial network organization towards a more fragmented conformation, as shown by our investigation on fibroblasts from four patients reported in the current and previous studies (Amati-Bonneau *et al.*, 2005), may also imply changes in the cristae organization and stabilization of mtDNA nucleoids, as well as their actual amount. Comparatively to other tissues, the skeletal muscle mitochondrial network is differently organized and specific studies investigating the fission/fusion activity in this tissue are lacking. Muscle cells are a syncytium with mitochondria being intercalated among the myofibres and abundantly located subsarcolemmally, the site where mitochondria increase in numbers when compensatory proliferation occurs in mitochondrial disorders. Our electron microscopy images of muscle mitochondria show some of the classical changes previously reported in mitochondrial myopathies, but these are most probably due to the accumulation of mtDNA deletions and not primarily generated by the OPA1 mutations.

The clinical presentation of our patients is similar to what is usually seen in other mitochondrial encephalomyopathies and more specifically in syndromes related to mtDNA multiple deletions. These cases widen the phenotypes that are associated with molecular defects in the OPA1 gene. The association of CPEO, mitochondrial myopathy with RRFs and COX negative fibres, cerebellar or spino-cerebellar involvement, and peripheral neuropathy has been all previously seen in patients with mutations in the POLG1 gene (Hudson and Chinnery, 2006). The only remarkable difference from these clinical phenotypes is the consistent presence of optic atrophy, as the core clinical manifestation of any OPA1-related phenotype. We propose that screening of the OPA1 gene in families with dominantly inherited CPEO and optic atrophy is mandatory, and only further screening of familial CPEO inherited as a mendelian trait without optic atrophy will provide evidence if the optic atrophy is a pathognomonic manifestation of OPA1-related disorders. It is of note that the only patient with a mutation lying outside the GTPase

domain (V910D, Family 2) had the milder phenotype characterized essentially by only optic atrophy as in classic DOA, but had evidence of myopathy. The latter had no clear morphologic signs of mitochondrial dysfunction at muscle histoenzymatic staining, such as RRFs or COX negative fibres, but had pathologically increased lactic acid after exercise, mitochondria with paracristalline inclusions at electron microscopy, and the lowest amount of mtDNA multiple deletions. Thus, contrary to the truncative mutations in the OPA1 gene predicted to lead to haploinsufficiency, which do not present a tight genotype–phenotype correlation, we suggest that with OPA1 mis-sense mutations the genotype may be associated with specific clinical phenotypes. However, it must be noted that a number of other mis-sense mutations in the OPA1 gene have been described and listed in the eOPA1 website (http://lbbma.univ-angers.fr) (Ferre *et al.*, 2005), including the exons building up the GTPase domain. Concerning these latter mutations there is no report of 'plus' features in these patients, which seem to be affected by classic DOA. Thus, it is reasonable to assume that mis-sense mutations in the GTPase domain not necessarily lead to 'OPA1 plus' phenotypes, which may be strictly dependent on amino acid location and/or change.

Overall, the involvement of OPA1 in mtDNA stability opens a wide and unexpected scenario, where all the other proteins involved in the machinery of mitochondrial fission/fusion may be implicated (Chen and Chan, 2005). The field of human disorders related to molecular defects in such proteins is rapidly growing, having at least other three examples besides OPA1 mutations in DOA: mutations in the *Mfn2* gene causing Charcot–Marie-Tooth (CMT) type 2A dominant peripheral neuropathy (Zuchner *et al.*, 2004), mutations in the *GDAP1* gene causing CMT4A (Niemann *et al.*, 2005), and the most recently reported first mutation in the *DLP1* gene associated with a lethal infantile neurological syndrome (Waterham *et al.*, 2007), all these disorders being frequently if not always associated with optic atrophy. A further confirmation that fission/fusion machinery may be very relevant for both mtDNA maintenance and integrity comes from recent studies on *Mfn1* and *Mfn2*, as well as *OPA1* null cells, suggesting loss of mtDNA nucleoids and defective oxidative phosphorylation (Chen *et al.*, 2007).

In conclusion, we report the novel implication of specific mis-sense mutations in the OPA1 gene in the maintenance of mtDNA integrity and the association with optic atrophy 'plus' syndromes, similar to classic mitochondrial encephalomyopathies. The mechanism leading to mtDNA multiple deletions is unclear and needs further investigations. However, the obvious consequence of this report is to consider *OPA1* gene analysis in patients with unexplained mitochondrial diseases, in particular if optic atrophy is present and mtDNA multiple deletions are recognized in the skeletal muscle.

Acknowledgements

This study has been supported by Telethon-Italy (grant# GGP06233 to V.C.), fondazione Gino Galletti (grant to V.C.), and progetto di ricerca sanitaria finalizzata (grant to V.C. and M.R.). P.A.B., P.R., D.B., A.B. and G.L. were supported by INSERM, the University Hospital of Angers (PHRC 04-12), the University of Angers and Montpellier I and II, France and by grants from Retina France and 'Ouvrir les yeux' patients Association. Further financial support comes from the Fondo de Investigaciones Sanitarias, Instituto de Salud Carlos III, Spain (PI060205 to B.B. and PI060547 to M.A.M.) and Ministerio de Educación y Ciencia, Spain (BFU2004-04591 to R.G.). We would like to thank Dr Luca Scorrano and Dr Arturo Carta for referring the Italian patients, and Dr Francesca Falzone, Dr Giulia Barcia, and Prof. Antonia Parmeggiani for their help in clinical management of the Italian patients. We are deeply indebted to all patients and their families for participating in this project. Funding to pay the Open Access publication charges for this article was provided by the RFO University of Bologna 2006 grant.

References

Alexander C, Votruba M, Pesch UE, Thiselton DL, Mayer S, Moore A, et al. OPA1, encoding a dynamin-related GTPase, is mutated in autosomal dominant optic atrophy linked to chromosome 3q28. Nat Genet 2000; 26: 211–5.

Amati-Bonneau P, Odent S, Derrien C, Pasquier L, Malthiery Y, Reynier P, et al. The association of autosomal dominant optic atrophy and moderate deafness may be due to the R445H mutation in the OPA1 gene. Am J Ophthalmol 2003; 136: 1170–1.

Amati-Bonneau P, Guichet A, Olichon A, Chevrollier A, Viala F, Miot S, et al. OPA1 R445H mutation in optic atrophy associated with sensorineural deafness. Ann Neurol 2005; 58: 958–63.

Andrews RM, Kubacka I, Chinnery PF, Lightowlers RN, Turnbull DM, Howell N. Reanalysis and revision of the Cambridge reference sequence for human mitochondrial DNA. Nat Genet 1999; 23: 147.

Bua E, Johnson J, Herbst A, Delong B, McKenzie D, Salamat S, et al. Mitochondrial DNA-deletion mutations accumulate intracellularly to detrimental levels in aged human skeletal muscle fibers. Am J Hum Genet 2006; 79: 469–80.

Carelli V, Ross-Cisneros FN, Sadun AA. Mitochondrial dysfunction as a cause of optic neuropathies. Prog Retin Eye Res 2004; 23: 53–89.

Chen H, Chan DC. Emerging functions of mammalian mitochondrial fusion and fission. Hum Mol Genet 2005; 14: R283–9.

Chen H, McCaffery JM, Chan DC. Mitochondrial fusion protects against neurodegeneration in the cerebellum. Cell 2007; 130: 548–62.

Cohn AC, Toomes C, Potter C, Towns KV, Hewitt AW, Inglehearn CF, et al. Autosomal dominant optic atrophy: penetrance and expressivity in patients with OPA1 mutations. Am J Ophthalmol 2007; 143: 656–62.

Cossarizza A, Riva A, Pinti M, Ammannato S, Fedeli P, Mussini C, et al. Increased mitochondrial DNA content in peripheral blood lymphocytes from HIV-infected patients with lipodystrophy. Antiviral Therapy 2003; 8: 51–7.

Delettre C, Lenaers G, Griffoin JM, Gigarel N, Lorenzo C, Belenguer P, et al. Nuclear gene OPA1, encoding a mitochondrial dynamin-related protein, is mutated in dominant optic atrophy. Nat Genet 2000; 26: 207–10.

Delettre C, Lenaers G, Pelloquin L, Belenguer P, Hamel CP. OPA1 (Kjer type) dominant optic atrophy: a novel mitochondrial disease. Mol Genet Metab 2002; 75: 97–107.

DiMauro S, Schon EA. Mitochondrial respiratory-chain diseases. N Engl J Med 2003; 348: 2656–68.

Ferre M, Amati-Bonneau P, Tourmen Y, Malthiery Y, Reynier P. eOPA1: an online database for OPA1 mutations. Hum Mutat 2005; 25: 423–8.

Frezza C, Cipolat S, Martins de Brito O, Micaroni M, Beznoussenko GV, Rudka T, et al. OPA1 controls apoptotic cristae remodeling independently from mitochondrial fusion. Cell 2006; 126: 177–89.

Ghelli A, Zanna C, Porcelli AM, Schapira AH, Martinuzzi A, Carelli V, et al. Leber's hereditary optic neuropathy (LHON) pathogenic mutations induce mitochondrial-dependent apoptotic death in transmitochondrial cells incubated with galactose medium. J Biol Chem 2003; 278: 4145–50.

González-Vioque E, Blazquez A, Fernández-Moreira D, Bornstein B, Bautista J, Arpa J, et al. Association of novel POLG mutations and mtDNA multiple deletions with variable clinical phenotypes in a Spanish population. Arch Neurol 2006; 63: 107–11.

Herlan M, Vogel F, Bornhovd C, Neupert W, Reichert AS. Processing of Mgm1 by the rhomboid-type protease Pcp1 is required for maintenance of mitochondrial morphology and of mitochondrial DNA. J Biol Chem 2003; 278: 27781–8.

Hirano M, Nishigaki Y, Marti R. Mitochondrial neurogastrointestinal encephalomyopathy (MNGIE): a disease of two genomes. Neurologist 2004; 10: 8–17.

Hoppins S, Lackner L, Nunnari J. The machine that divide and fuse mitochondria. Ann Rev Biochem 2007; 76: 33.1–.30.

Hudson G, Chinnery PF. Mitochondrial DNA polymerase-gamma and human disease. Hum Mol Genet 2006; 15 (Spec No 2): R244–52.

Hudson G, Amati-Bonneau P, Blakely EL, Stewart JD, He L, Schaefer AM, et al. Mutation of *OPA1* causes dominant optic atrophy with external ophthalmoplegia, ataxia, deafness and multiple mitochondrial DNA deletions: a novel disorder of mtDNA maintenance. Brain 2007.

Jaroszewski L, Li W, Godzik A. In search for more accurate alignments in the twilight zone. Protein Sci 2002; 11: 1702–13.

Johnston W, Karpati G, Carpenter S, Arnold D, Shoubridge EA. Late-onset mitochondrial myopathy. Ann Neurol 1995; 37: 16–23.

Kaukonen J, Juselius JK, Tiranti V, Kyttala A, Zeviani M, Comi GP, et al. Role of adenine nucleotide translocator 1 in mtDNA maintenance. Science 2000; 289: 782–5.

Kim JY, Hwang JM, Ko HS, Seong MW, Park BJ, Park SS. Mitochondrial DNA content is decreased in autosomal dominant optic atrophy. Neurology 2005; 64: 966–72.

Kjer P. Infantile optic atrophy with dominant mode of inheritance: a clinical and genetic study of 19 Danish families. Acta Ophthalmol Scand 1959; 37: 1–146.

Liguori M, La Russa A, Manna I, Andreoli V, Caracciolo M, Spadafora P, et al. A phenotypic variation of dominant optic atrophy and deafness (ADOAD) due to a novel OPA1 mutation. J Neurol (in press).

Lodi R, Tonon C, Valentino ML, Iotti S, Clementi V, Malucelli E, et al. Deficit of in vivo mitochondrial ATP production in OPA1-related dominant optic atrophy. Ann Neurol 2004; 56: 719–23.

Low HH, Lowe J. A bacterial dynamin-like protein. Nature 2006; 444: 766–9.

Malka F, Lombes A, Rojo M. Organization, dynamics and transmission of mitochondrial DNA: focus on vertebrate nucleoids. Biochim Biophys Acta 2006; 1763: 463–72.

Meire F, De Laey JJ, de Bie S, van Staey M, Matton MT. Dominant optic nerve atrophy with progressive hearing loss and chronic progressive external ophthalmoplegia (CPEO). Ophthalmic Paediatr Genet 1985; 5: 91–7.

Moraes CT, DiMauro S, Zeviani M, Lombes A, Shanske S, Miranda AF, et al. Mitochondrial DNA deletions in progressive external ophthalmoplegia and Kearns-Sayre syndrome. N Engl J Med 1989; 320: 1293–9.

Nakamura M, Lin J, Ueno S, Asaoka R, Hirai T, Hotta Y, et al. Novel mutations in the OPA1 gene and associated clinical features in Japanese patients with optic atrophy. Ophthalmology 2006; 113: 483–8.

Niemann A, Ruegg M, La Padula V, Schenone A, Suter U. Ganglioside-induced differentiation associated protein 1 is a regulator of the mitochondrial network: new implications for Charcot-Marie-Tooth disease. J Cell Biol 2005; 170: 1067–78.

Nishigaki Y, Marti R, Hirano M. ND5 is a hot-spot for multiple atypical mitochondrial DNA deletions in mitochondrial neurogastrointestinal encephalomyopathy. Hum Mol Genet 2004; 13: 91–101.

Nishino I, Spinazzola A, Hirano M. Thymidine phosphorylase gene mutations in MNGIE, a human mitochondrial disorder. Science 1999; 283: 689–92.

Olichon A, Baricault L, Gas N, Guillou E, Valette A, Belenguer P, et al. Loss of OPA1 perturbates the mitochondrial inner membrane structure and integrity, leading to cytochrome c release and apoptosis. J Biol Chem 2003; 278: 7743–6.

Olichon A, Guillou E, Delettre C, Landes T, Arnauné-Pelloquin L, Emorine LJ, et al. Mitochondrial dynamics and disease, OPA1. Biochim Biophys Acta 2006; 1763: 500–9.

Payne M, Yang Z, Katz BJ, Warner JE, Weight CJ, Zhao Y, et al. Dominant optic atrophy, sensorineural hearing loss, ptosis, and ophthalmoplegia: a syndrome caused by a missense mutation in OPA1. Am J Ophthalmol 2004; 138: 749–55.

Pesch UE, Leo-Kottler B, Mayer S, Jurklies B, Kellner U, Apfelstedt-Sylla E, et al. OPA1 mutations in patients with autosomal dominant optic atrophy and evidence for semi-dominant inheritance. Hum Mol Genet 2001; 10: 1359–68.

Praefcke GJK, McMahon HT. The dynamin superfamily: universal membrane tubulation and fission molecules? Nat Rev 2004; 5: 133–47.

Shimizu S, Mori N, Kishi M, Sugata H, Tsuda A, Kubota N. A novel mutation in the OPA1 gene in a Japanese patient with optic atrophy. Am J Ophthalmol 2003; 135: 256–7.

Spelbrink JN, Li FY, Tiranti V, Nikali K, Yuan QP, Tariq M, et al. Human mitochondrial DNA deletions associated with mutations in the gene encoding Twinkle, a phage T7 gene 4-like protein localized in mitochondria. Nat Genet 2001; 28: 223–31.

Staden R, Beal KF, Bonfield JK. The Staden package, 1998. Methods Mol Biol 2000; 132: 115–30.

Treft RL, Sanborn GE, Carey J, Swartz M, Crisp D, Wester DC, et al. Dominant optic atrophy, deafness, ptosis, ophthalmoplegia, dystaxia, and myopathy. A new syndrome. Ophthalmology 1984; 91: 908–15.

Van Goethem G, Dermaut B, Lofgren A, Martin JJ, Van Broeckhoven C. Mutation of POLG is associated with progressive external ophthalmoplegia characterized by mtDNA deletions. Nat Genet 2001; 28: 211–2.

Waterham HR, Koster J, van Roermund CW, Mooyer PA, Wanders RJ, Leonard JV. A lethal defect of mitochondrial and peroxisomal fission. N Engl J Med 2007; 356: 1736–41.

Zeviani M, Servidei S, Gellera C, Bertini E, DiMauro S, DiDonato S. An autosomal dominant disorder with multiple deletions of mitochondrial DNA starting at the D-loop region. Nature 1989; 339: 309–11.

Zuchner S, Mersiyanova IV, Muglia M, Bissar-Tadmouri N, Rochelle J, Dadali EL. Mutations in the mitochondrial GTPase mitofusin 2 cause Charcot-Marie-Tooth neuropathy type 2A. Nat Genet 2004; 36: 449–51.